

SCIENTIFIC REPORTS



OPEN

Functional characterization of *ent*-copalyl diphosphate synthase, kaurene synthase and kaurene oxidase in the *Salvia miltiorrhiza* gibberellin biosynthetic pathway

Received: 29 October 2015
Accepted: 24 February 2016
Published: 14 March 2016

Ping Su^{1,2,*}, Yuru Tong^{1,2,*}, Qiqing Cheng^{1,2,3}, Yating Hu⁴, Meng Zhang¹, Jian Yang², Zhongqiu Teng², Wei Gao¹ & Luqi Huang²

Salvia miltiorrhiza Bunge is highly valued in traditional Chinese medicine for its roots and rhizomes. Its bioactive diterpenoid tanshinones have been reported to have many pharmaceutical activities, including antibacterial, anti-inflammatory, and anticancer properties. Previous studies found four different diterpenoid biosynthetic pathways from the universal diterpenoid precursor (*E,E,E*-geranylgeranyl diphosphate (GGPP) in *S. miltiorrhiza*. Here, we describe the functional characterization of *ent*-copalyl diphosphate synthase (SmCPS_{ent}), kaurene synthase (SmKS) and kaurene oxidase (SmKO) in the gibberellin (GA) biosynthetic pathway. SmCPS_{ent} catalyzes the cyclization of GGPP to *ent*-copalyl diphosphate (*ent*-CPP), which is converted to *ent*-kaurene by SmKS. Then, SmKO catalyzes the three-step oxidation of *ent*-kaurene to *ent*-kaurenoic acid. Our results show that the fused enzyme SmKS-SmCPS_{ent} increases *ent*-kaurene production by several fold compared with separate expression of SmCPS_{ent} and SmKS in yeast strains. In this study, we clarify the GA biosynthetic pathway from GGPP to *ent*-kaurenoic acid and provide a foundation for further characterization of the subsequent enzymes involved in this pathway. These insights may allow for better growth and the improved accumulation of bioactive tanshinones in *S. miltiorrhiza* through the regulation of the expression of these genes during developmental processes.

Salvia miltiorrhiza Bunge has been widely used in China (and to a lesser extent in Japan, the United States, and European countries) for the treatment of cardiovascular and cerebrovascular diseases. This medicinal herb exhibits anti-inflammatory, antioxidant and radical scavenging effects^{1,2}. Tanshinone I, tanshinone IIA, cryptotanshinone and dihydrotanshinone I are the major diterpene quinones of the lipophilic constituents in Danshen and are responsible for much of its anti-inflammatory, antioxidant, antitumor and a variety of other activities^{3–5}. Because these monomeric compounds have significant pharmacological activities, Danshen preparations are more frequently used in the clinic.

To accommodate the increasing need for clinical applications, researchers have deeply investigated the diterpenoid biosynthetic pathway to obtain the bioactive tanshinones directly using synthetic biology strategies in microbial cell factories. Previous works have indicated that at least four different diterpenoid biosynthetic pathways exist in *S. miltiorrhiza* (Fig. 1)⁶. Among them, the tanshinone biosynthetic pathway is uniquely initiated by a sequential pair of cyclization reactions catalyzed by SmCPS1 and SmKSL1 to produce abietane miltiradiene,

¹School of Traditional Chinese Medicine, Capital Medical University, Beijing, China. ²State Key Laboratory Breeding Base of Dao-di Herbs, National Resource Center for Chinese Materia Medica, China Academy of Chinese Medical Sciences, Beijing, China. ³State Key Laboratory of Quality Research in Chinese Medicine, Macau University of Science and Technology, Avenida Wai Long, Taipa, Macau, China. ⁴Department of Chemical and Biological Engineering, Chalmers University of Technology, Kemivägen 10, SE-41296 Göteborg, Sweden. *These authors contributed equally to this work. Correspondence and requests for materials should be addressed to W.G. (email: weigao@cmmu.edu.cn) or L.H. (email: huangluqi01@126.com)

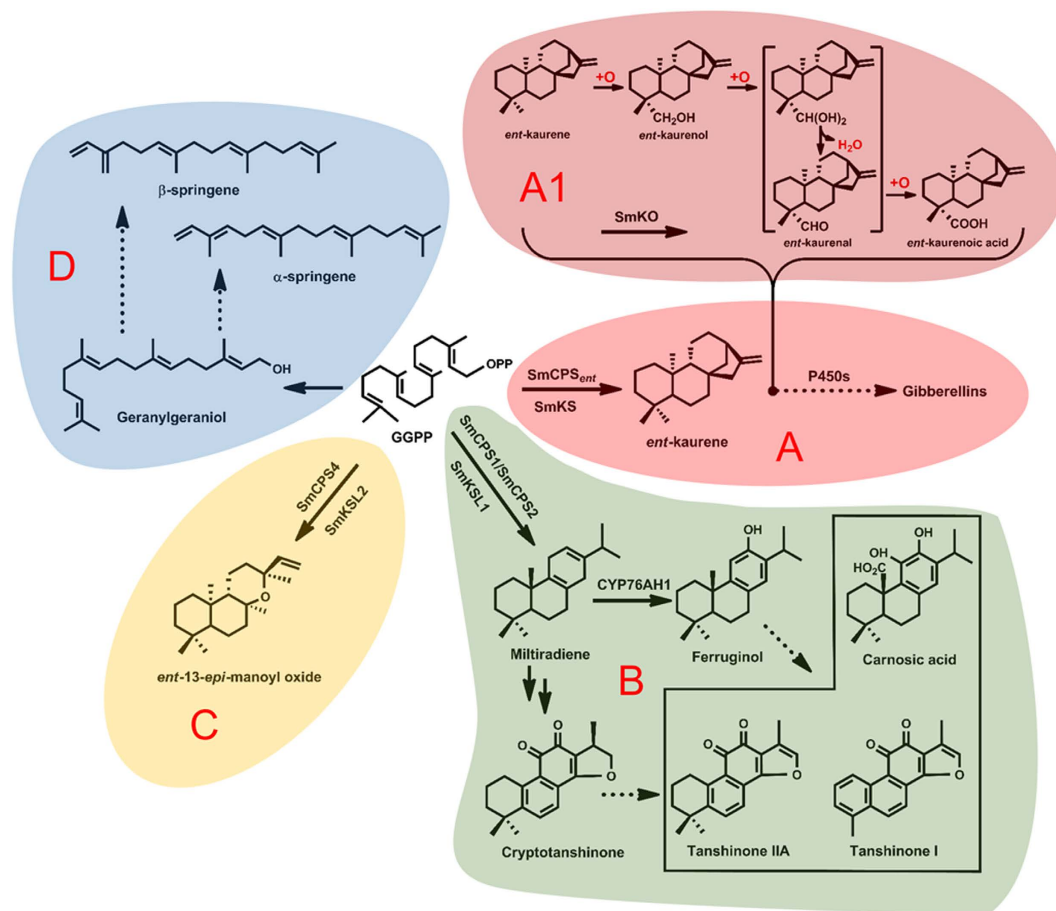


Figure 1. Four different diterpenoid biosynthetic pathways in *S. miltiorrhiza*. (A) Gibberellin biosynthetic pathway. (A1) Proposed mechanism for SmKO conversion of *ent*-kaurene into *ent*-kaurenoic acid³⁵. (B) Tanshinone biosynthetic pathway. (C,D) Unknown diterpenoid biosynthetic pathways.

which is a precursor of at least cryptotanshinone^{7,8}. Then, SmCYP76AH1 catalyzes the turnover of miltiradiene to form ferruginol, thereby providing a solid foundation to elucidate the tanshinone biosynthetic pathway.

However, only two diterpene synthases (diTPSs) in the *S. miltiorrhiza* GA biosynthetic pathway have been reported to date, and the roles of GAs in *S. miltiorrhiza* root and rhizome development and the total yield of tanshinones per plant are less clear. GAs are formed from GGPP via a set of reactions catalyzed by different enzymes, including two consecutive diTPSs, cytochrome P450 (CYP) and 2-oxoglutarate-dependent dioxygenases (2ODDs) in plants⁹. As a group of plant-growth regulators, these GAs control different aspects of plant development, such as seed germination, stem elongation, flowering, fruit set and fruit development. Understanding GA biosynthesis will allow us to improve the tanshinone contents by regulating the expression of the genes involved in the *S. miltiorrhiza* GA biosynthetic pathway. Here, we cloned three genes (*SmCPS_{ent}*, *SmKS* and *SmKO*) from *S. miltiorrhiza* hairy roots and then identified their functions by co-expressing them in *Saccharomyces cerevisiae*. Biochemical studies suggested that CPS and KS might interact with one another¹⁰; therefore, we constructed a fused *SmCPS_{ent}* and *SmKS* protein and showed that the production of *ent*-kaurene was significantly improved.

Results

Cloning and sequence analysis of *SmCPS_{ent}*, *SmKS* and *SmKO* from *S. miltiorrhiza* hairy roots.

The full-length *SmCPS_{ent}* and *SmKS* cDNAs were determined by 5' RACE and 3' RACE, and the corresponding cDNA sequences were submitted to the National Center for Biotechnology Information (Supplementary Fig. S1). The full-length *SmCPS_{ent}* cDNA (GenBank accession number KT934789) is 2413 nt and encodes a polypeptide of 793 amino acids. *SmCPS_{ent}* clusters most closely to *SmCPS5* of *S. miltiorrhiza* f. *alba* and to *SdCPS* from *Scoparia dulcis* (Fig. 2). The first 21 N-terminal amino acids are rich in serine and threonine (19%), which is a common characteristic of transit peptides that target the diTPS to plastids^{11,12}. This information was supported by our analysis using ChloroP 1.1¹³. The amino acid sequence also contains a conserved DIDD motif (Fig. 3), which strongly suggests that *SmCPS_{ent}* can catalyze GGPP to CPP as a class II diTPS. The *SmKS* cDNA (GenBank accession number KT934790) is 2636 nt in length and encodes a predicted protein of 806 amino acid residues. At the protein level, the KS sequence from the hairy roots of *S. miltiorrhiza* exhibits 99% identity with the *SmKSL2* from *S. miltiorrhiza* f. *alba* (Fig. 2). The first 27 N-terminal amino acids are rich in serine and threonine (22%), suggesting that *SmKS* is also localized in plastids. Its amino acid sequence contains a DDFFD motif but lacks the

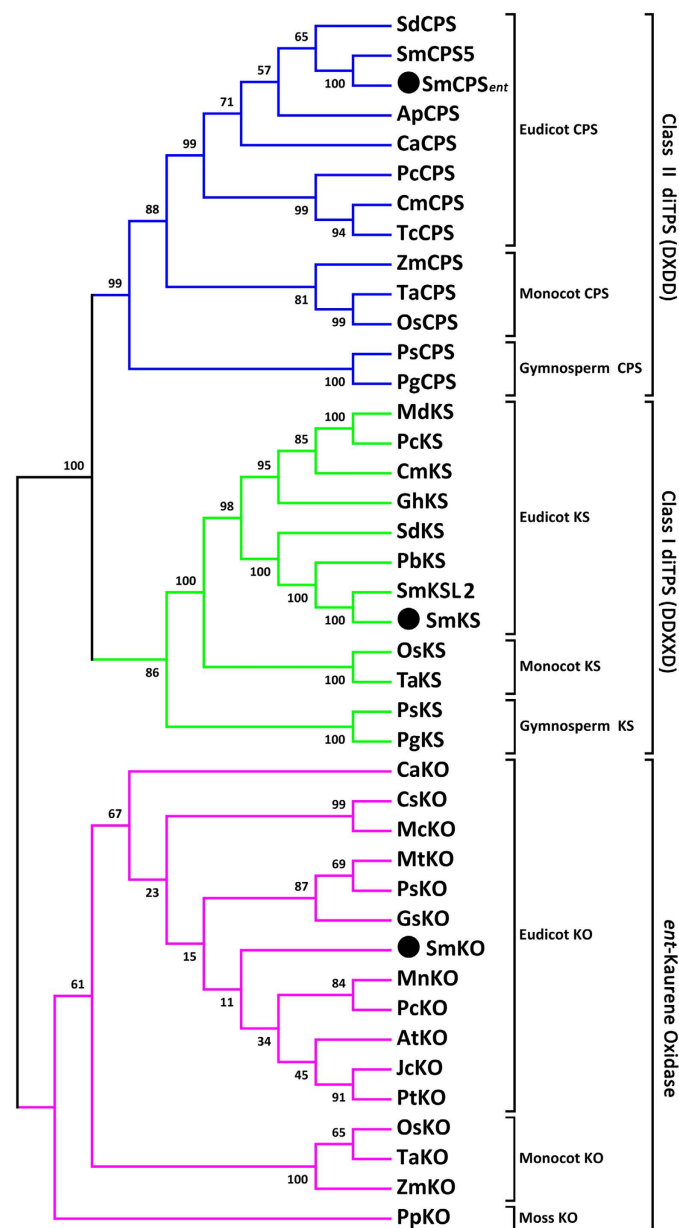


Figure 2. Phylogenetic tree of CPS, KS and KO from different species. The neighbor-joining phylogenetic trees were constructed using the bootstrap method in MEGA 5.1. The number of bootstrap replications was 1000. Descriptions of the three different types of synthases used in the phylogeny are listed in Supplementary Table 2.

DxDD motif (Fig. 3), indicating that SmKS is a plant KS protein with monofunctional class I diTPS activity. The *SmKO* cDNA (GenBank accession number KJ606394) is 1930 nt in length and has an open reading frame (ORF) encoding 519 amino acid residues, containing a cytochrome P450 conserved site (amino acids 451–460, Fig. 3). The deduced amino acid sequence shows 64% and 66% identity with *AtKO* (*Arabidopsis thaliana*, AAC39507) and *PsKO* (*Pisum sativum*, AAP69988) (Fig. 2). The gene was identified as a multifunctional kaurene oxidase catalyzing three sequential oxidations (*ent*-kaurene to *ent*-kaurenoic acid) in the GA biosynthetic pathway^{14,15}.

Recombinant expression and functional characterization of SmCPS_{ent} and SmKS. Previously reported evidence suggested that SmCPS_{ent} and SmKS might be involved in the *S. miltiorrhiza* GA biosynthetic pathway⁶. To confirm the biochemical functions of SmCPS_{ent} and SmKS *in vivo*, the SmCPS_{ent} ORF and SmKS ORFs were ligated individually or in combination in the yeast expression vector pESC-Trp (Fig. 4A) and expressed in the yeast strain BY-T20 (provided by Prof. Xueli Zhang's lab, Tianjin Institute of Industrial Biotechnology, Chinese Academy of Sciences, China). As expected, CPP was detected as the SmCPS_{ent} product

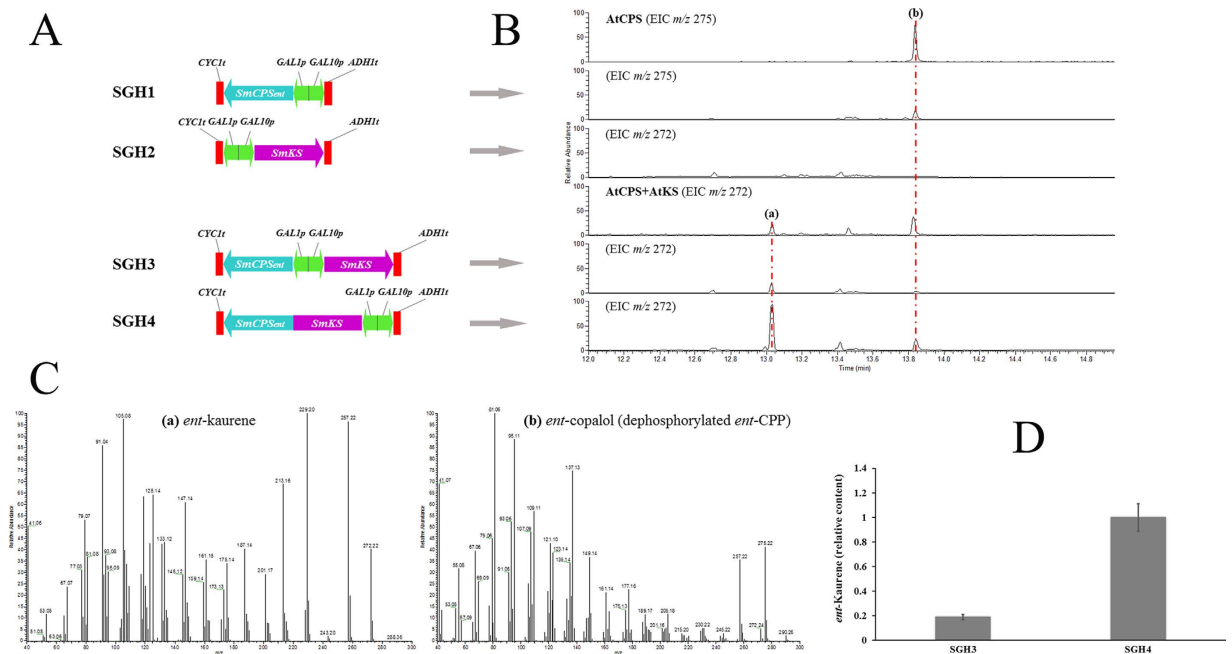


Figure 4. Extracts from yeast strain BY-T20 cultures expressing the *S. miltiorrhiza* *SmCPS_{ent}* or/and *SmKS* using GC-MS. (A) Construction of the recombinant plasmid in yeast strains. BY-T20: BY4742, $\Delta Trp1$, *Trp1::HIS3-P_{PGK1}-BTS1/ERG20-T_{ADHI}-P_{TDH3}-SaGGPS-T_{TPH1}-P_{TEF1}-tHMG1-T_{CYC1}*. SGH1: BY-T20/pESC-Trp::*SmCPS_{ent}*. SGH2: BY-T20/pESC-Trp::*SmKS*, SGH3: BY-T20/pESC-Trp::*SmCPS_{ent}*/*SmKS*, SGH4: BY-T20/pESC-Trp::*SmKS*-*SmCPS_{ent}*. (B) Extracted ion chromatograms showing the *SmCPS_{ent}* and *SmKS* products. *AtCPS* (*ent*-copalol, the dephosphorylated product of *ent*-CPP), *AtCPS* + *AtKS* (*ent*-kaurene). (C) The mass spectra of the *SmCPS_{ent}* and *SmKS* products. (D) Relative *ent*-kaurene contents in the yeast strains SGH3 and SGH4 based on their peak area ratio. The data represent the mean \pm SD from three independent experiments.

vector. Using the product of the *A. thaliana* *AtKS* as the authentic standard, *ent*-kaurene was detected as the *SmKS* product in the products of the yeast strain SGH3 (BY-T20/pESC-Trp::*SmCPS_{ent}*/*SmKS*) but not SGH2 (BY-T20/pESC-Trp::*SmKS*), confirming that *SmKS* possessed monofunctional class I diTPS activity and catalyzed the formation of *ent*-kaurene using the *SmCPS_{ent}* product CPP as the substrate. Therefore, the absolute configuration of the *SmCPS_{ent}* product CPP was identified as an enantiomer (i.e., *ent*-CPP) (Fig. 4B).

Protein complexes have been reported to improve the efficiency of specific pathways by protecting substrates and intermediates from diffusion and degradation¹⁶. Zhou *et al.* reported that a recombinant strain containing the fused enzyme *SmKSL1-SmCPS1* produced 2.8-fold more miltradiene compared with another recombinant strain in which *SmCPS1* and *SmKSL1* were expressed separately¹⁷. Hence, we constructed the fused enzyme *SmKS-SmCPS_{ent}* in the yeast strain SGH4 (BY-T20/pESC-Trp::*SmKS-SmCPS_{ent}*) using the RF cloning method, and the results showed that SGH4 produced approximately 4.25-fold more *ent*-kaurene than SGH3 (Fig. 4D).

Recombinant expression and functional characterization of *SmKO* in vivo. As a strategy to characterize the biochemical function of *SmKO* in vivo, first we constructed the fused enzyme *SmKS-SmCPS_{ent}*, which improved the *ent*-kaurene precursor supply as expected. Then, *SmKO* was coexpressed with the fused enzyme *SmKS-SmCPS_{ent}* and a NADPH-cytochrome P450 reductase (*SmCPR1*) in the yeast strain SGH5 (BY-T20/pESC-Trp::*SmKS-SmCPS_{ent}*/*SmKO* + pESC-Leu::*SmCPR1*). After extraction and methylation, the *ent*-kaurenoic acid methyl ester was detected by a comparison with the methylated authentic standard (Sigma, USA) (Fig. 5). This result confirmed that *SmKO* encoded a functional *ent*-kaurene oxidase that was involved in the three-stage oxidation of *ent*-kaurene to *ent*-kaurenoic acid in the *S. miltiorrhiza* GA biosynthetic pathway.

Discussion

We identified three consecutive enzymes (*SmCPS_{ent}*, *SmKS* and *SmKO*) involved in the *S. miltiorrhiza* GA biosynthetic pathway. *SmCPS_{ent}* catalyzes the formation of *ent*-CPP from GGPP; then, *SmKS* converts *ent*-CPP to *ent*-kaurene. Subsequently, *SmKO* converts *ent*-kaurene to *ent*-kaurenoic acid via a three-stage oxidation reaction. *ent*-Kaurene biosynthesis was reported to be catalyzed by a one-to-one CPS/KS complex in which CPP could be channeled from CPS to the KS catalytic site¹⁰. Therefore, we fused *SmCPS_{ent}* and *SmKS* to obtain a close proximity between the active sites of the two consecutive enzymes. As expected, the fused enzyme *SmKS-SmCPS_{ent}* produced 4.25-fold more *ent*-kaurene than the separate expression of *SmCPS_{ent}* and *SmKS* in the yeast strain, suggesting that the protein fusion treatment was an efficient approach to improve the catalytic activity and enlarge the heterologous production of *ent*-kaurene. With an increased supply of the *ent*-kaurene precursor, *SmKO* catalyzed the formation of *ent*-kaurenoic acid. However, the intermediates *ent*-kaurenol and *ent*-kaurenal were not detected. One possible explanation is that the intermediates were unstable and were changed into other

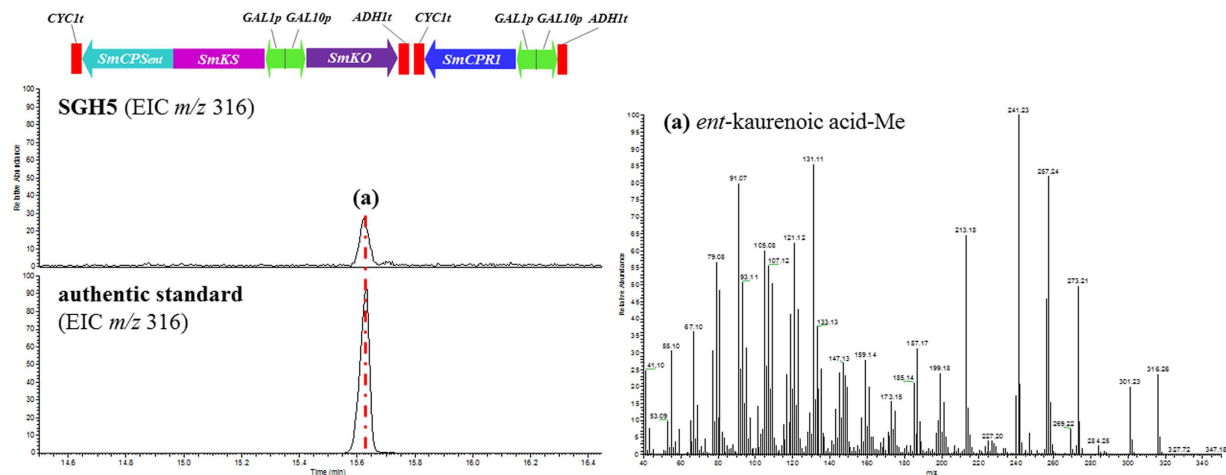


Figure 5. The product from BY-T20 yeast strains expressing the *S. miltiorrhiza* *SmKO*. SGH5: BY-T20/pESC-Trp::SmKS-SmCPS_{ent}/SmKO + pESC-Leu::SmCPR1. Extracted ion chromatograms showing methyl ester derivatives of the *SmKO* product with its corresponding mass spectra.

intermediates during the extraction process. The enzymes involved in the early steps of the GA biosynthetic pathway (i.e., CPS, KS, KO, and KAO) are primarily encoded by single genes, whereas those involved in the later steps (i.e., GA20ox, GA3ox, and GA2ox) are encoded by gene families¹⁸. The *SmCPS_{ent}*, *SmKS* and *SmKO* genes are likely single copy genes responsible for GA biosynthesis in *S. miltiorrhiza*.

In addition to the identification and characterization of *SmCPS_{ent}*, *SmKS* and *SmKO*, we provided insights into the genes encoding the enzymes involved in all steps of the GA biosynthetic pathway from GGPP to *ent*-kaurenoic acid. Our results provide a foundation for further characterization of the subsequent enzymes (i.e., *SmKAO* and the CYP88A subfamily) involved in the GA biosynthetic pathway using this yeast expression system. In plants, GA levels vary at different sites and during different development processes¹⁹. It is possible to control the GA levels by regulating the expression of these genes to acquire better growth of the *S. miltiorrhiza* roots and rhizomes, thereby improving the total yield of tanshinones per plant.

In conclusion, we functionally characterized three consecutive enzymes (*SmCPS_{ent}*, *SmKS* and *SmKO*) involved in the GA biosynthetic pathway from GGPP to *ent*-kaurenoic acid, thereby laying the foundation for further characterization of GA biosynthesis. Based on these results, we could regulate the expression of all genes involved in the GA biosynthetic pathway to acquire better growth and an increased accumulation of the bioactive tanshinones involved in the *S. miltiorrhiza* developmental processes. Protein fusion is an applicable and efficient approach that can be used to direct metabolic flux to the bioactive diterpenoid tanshinones pathway for the heterologous production of isoprenoids in microbial cell factories.

Methods

RNA isolation and cDNA cloning. Hairy roots were induced from the *S. miltiorrhiza* leaf explants under the mediation of *A. rhizogenes* strain ACCC10060 as described previously²⁰ and maintained in 6,7-V liquid medium²¹ at 25 °C on a gyratory shaker (80 rpm) in the dark. Total RNA was extracted using the TRIzol reagent (Invitrogen, Carlsbad, CA, USA). The 5' and 3' ends of the targeted *SmCPS_{ent}* and *SmKS* genes were cloned by RACE (Invitrogen) according to the manufacturer's directions using the corresponding *S. miltiorrhiza* genome sequences released by the National Center for Biotechnology Information (NCBI)²². The primer sequences are shown in Supplementary Table 1. An aliquot (1 µg) of the total RNA was used to synthesize the first strand cDNA according to the PrimeScript 1st Strand cDNA Synthesis Kit (Takara Bio, Dalian, China) manufacturer's protocol. The full-length cDNA for each ORF was cloned using the PrimeSTAR DNA polymerase (Takara Bio). The PCR products were purified and cloned into the pEASY-T3 cloning vector (TransGen Biotech, Beijing, China), transformed into *Escherichia coli* Trans5α cells (TransGen Biotech), and then cultured in Luria-Bertani (LB) medium at 37 °C in the dark. Positive clones were sequenced. The full-length cDNA of *SmKO* was cloned previously²³.

Bioinformatics analysis. The *SmCPS_{ent}*, *SmKS* and *SmKO* sequences were confirmed at NCBI (<http://www.ncbi.nlm.nih.gov/>). The open reading frames (ORFs) and deduced amino acid sequences were analyzed using the online tool ORF Finder (<http://www.ncbi.nlm.nih.gov/gorf/gorf.html>) and the ExPASy online tool (<http://web.expasy.org/translate/>), respectively. The ChloroP 1.1 Server (<http://www.cbs.dtu.dk/services/ChloroP/>) was used to predict chloroplast transit peptides. The sequences of the *SmCPS_{ent}*, *SmKS* and *SmKO* as well as other corresponding sequences downloaded from GenBank were aligned using the DNAMAN program, and the phylogenetic trees for *SmCPS_{ent}*, *SmKS* and *SmKO* were constructed using sequences from other plants (Supplementary Table 2) using the neighbor-joining method in MEGA5.1²⁴.

Recombinant expression and functional characterization of *SmCPS_{ent}* and *SmKS*. The *SmCPS_{ent}* and *SmKS* ORFs (alone or in combination) were subcloned into the yeast epitope-tagging vector pESC-Trp under the control of the GAL1 or GAL10 inducible promoter (Agilent Technologies, USA) via digestion by the

corresponding restriction endonucleases. The resulting constructs were verified by complete gene sequencing and then transformed into the yeast strain BY-T20 (BY4742, $\Delta Trp1$, $Trp1::HIS3-P_{PGK1}-BTS1/ERG20-T_{ADH1}-P_{TDH3}-SaGGPS-T_{TPI1}-P_{TEF1}-tHMG1-T_{CYC1}$, provided by Prof. Xueli Zhang's lab, Tianjin Institute of Industrial Biotechnology, Chinese Academy of Sciences, China)^{25–27}. Then, the recombinant strains SGH1 (containing the plasmid pESC-Trp::SmCPS_{ent}), SGH2 (containing the plasmid pESC-Trp::SmKS), and SGH3 (containing the plasmid pESC-Trp::SmCPS_{ent}/SmKS) were selected on synthetic dropin medium -Trp-His (SD-Trp-His) containing 20 g/L glucose and grown at 30 °C for 2–3 d. Single transformed yeast colonies were grown in SD-Trp-His liquid medium supplemented with 20 g/L glucose at 30 °C for approximately 2 d. The yeast cells were pelleted and resuspended in 100 mL of SD-Trp-His liquid induction medium supplemented with 20 g/L galactose and grown at 30 °C for 3 d. Finally, the induced yeast cells were extracted three times with an equal volume of hexane. The organic fractions were pooled and dried using a Nitrogen Evaporator (Baojingkeji, Henan, China). The dried samples were dissolved in 100 μ L of hexane for GC-MS analysis as described previously²⁸. To confirm the products of these strains, the identified products *ent*-CPP and *ent*-kaurene of *A. thaliana* AtCPS and AtKS were used as the authentic standards^{29,30}. The detailed protocols for the constructions of the recombinant plasmids and strains and the recombinant expression and enzymatic assay for AtCPS and AtKS are described in the Supplementary Methods.

Construction of the module producing the fused protein SmKS-SmCPS_{ent} and the functional characterization of SmKO.

To prepare the module producing the fused protein SmKS-SmCPS_{ent}, a restriction-free (RF) cloning method was used³¹. The genes encoding the fusion enzyme were constructed by inserting a widely used GGS linker encoded by a “GGT GGT GGT TCT” sequence between the two corresponding genes^{32,33}. The recombinant plasmid pESC-Trp::SmKS-SmCPS_{ent} was transformed into the yeast strain BY-T20 to generate SGH4 and induced with D-galactose as described above. Then, the products of SGH4 were analyzed by GC-MS. The detailed protocols for the RF cloning are described in the Supplementary Methods.

The ORF region of SmKO was ligated into the recombinant plasmid pESC-Trp::SmKS-SmCPS_{ent} as described above and then transformed into the yeast strain BY-T20 with another recombinant plasmid pESC-Leu::SmCPR1 (SmCPR1, *S. miltiorrhiza* cytochrome P450 reductase⁸). The recombinant strain SGH5 (containing the plasmids pESC-Trp::SmKS-SmCPS_{ent}/SmKO and pESC-Leu::SmCPR1) was induced with D-galactose and extracted once with an equal volume of hexane and twice with an equal volume of ethyl acetate. The organic fractions were pooled and dried and then dissolved in 50 μ L of methanol and methylated with approximately 200 μ L of (trimethylsilyl)diazomethane (Aladdin Industrial Inc., Shanghai, China). The methylated samples were redried and then dissolved in 100 μ L of ethyl acetate for GC-MS using a Thermo TRACE 1310/TSQ 8000 gas chromatograph (splitless; injector temperature 250 °C) with a DB-5 ms (30 m \times 0.25 mm \times 0.25 μ m) capillary column. The GC conditions were the same as those described previously³⁴.

References

- Jiang, W. Y. *et al.* PF2401-SF, standardized fraction of *Salvia miltiorrhiza* shows anti-inflammatory activity in macrophages and acute arthritis *in vivo*. *Int Immunopharmacol* **16**, 160–164 (2013).
- Kim, S. J., Kwon, D. Y., Kim, Y. S. & Kim, Y. C. Peroxyl radical scavenging capacity of extracts and isolated components from selected medicinal plants. *Arch Pharm Res* **33**, 867–873 (2010).
- Wang, S. *et al.* Tanshinone I selectively suppresses pro-inflammatory genes expression in activated microglia and prevents nigrostriatal dopaminergic neurodegeneration in a mouse model of Parkinson's disease. *J Ethnopharmacol* **164**, 247–255 (2015).
- Munagala, R., Aqil, F., Jayabalan, J. & Gupta, R. C. Tanshinone IIA inhibits viral oncogene expression leading to apoptosis and inhibition of cervical cancer. *Cancer Lett* **356**, 536–546 (2015).
- Cong, M. *et al.* Cryptotanshinone and dihydrotanshinone I exhibit strong inhibition towards human liver microsomal (HLM)-catalyzed propofol glucuronidation. *Fitoterapia* **85**, 109–113 (2013).
- Cui, G. H. *et al.* Functional divergence of diterpene syntheses in the medicinal plant *Salvia miltiorrhiza* Bunge. *Plant Physiol* **169**, 1607–1618 (2015).
- Gao, W. *et al.* A functional genomics approach to tanshinone biosynthesis provides stereochemical insights. *Org Lett* **11**, 5170–5173 (2009).
- Guo, J. *et al.* CYP76AH1 catalyzes turnover of miltiradiene in tanshinones biosynthesis and enables heterologous production of ferruginol in yeasts. *Proc Natl Acad Sci USA* **110**, 12108–12113 (2013).
- Hedden, P. *et al.* Gibberellin biosynthesis in plants and fungi: a case of convergent evolution? *J Plant Growth Regul* **20**, 319–331 (2001).
- Duncan, J. D. & West C. A. Properties of kaurene synthetase from *Marah macrocarpus* endosperm. Evidence for the participation of separate but interacting enzymes. *Plant Physiol* **68**, 1128–1134 (1981).
- Cho, E. *et al.* Molecular cloning and characterization of a cDNA encoding *ent*-cassa-12,15-diene synthase, a putative diterpenoid phytoalexin biosynthetic enzyme, from suspension-cultured rice cells treated with a chitin elicitor. *Plant J* **37**, 1–8 (2004).
- Günnewich, N. *et al.* A diterpene synthase from the clary sage *Salvia sclarea* catalyzes the cyclization of geranylgeranyl diphosphate to (8R)-hydroxy-copalyl diphosphate. *Phytochemistry* **91**, 93–99 (2013).
- Emanuelsson, O., Nielsen, H. & von Heijne, G. ChloroP, a neural network-based method for predicting chloroplast transit peptides and their cleavage sites. *Protein Sci* **8**, 978–984 (1999).
- Helliwell, C. A., Poole, A., Peacock, W. J. & Dennis, E. S. Arabidopsis *ent*-kaurene oxidase catalyzes three steps of gibberellin biosynthesis. *Plant Physiol* **119**, 507–510 (1999).
- Davidson, S. E., Smith, J. J., Helliwell, C. A., Poole, A. T. & Reid, J. B. The pea gene *LH* encodes *ent*-kaurene oxidase. *Plant Physiol* **134**, 1123–1134 (2004).
- Srere, P. A. Complexes of sequential metabolic enzymes. *Annu Rev Biochem* **56**, 89–124 (1987).
- Zhou, Y. J. *et al.* Modular pathway engineering of diterpenoid synthases and the mevalonic acid pathway for miltiradiene production. *J Am Chem Soc* **134**, 3234–3241 (2012).
- Sakamoto, T. *et al.* An overview of gibberellin metabolism enzyme genes and their related mutants in rice. *Plant Physiol* **134**, 1642–1653 (2004).
- Rebers, M. *et al.* Regulation of gibberellin biosynthesis genes during flower and early fruit development of tomato. *Plant J* **17**, 241–250 (1999).

20. Cheng, Q. Q. *et al.* RNA interference-mediated repression of *SmCPS* (copalyl diphosphate synthase) expression in hairy roots of *Salvia miltiorrhiza* causes a decrease of tanshinones and sheds light on the functional role of *SmCPS*. *Biotechnol Lett* **36**, 363–369 (2014).
21. Veliky, I. A. & Martin, S. M. A fermenter for plant cell suspension cultures. *Can J Microbiol* **16**, 223–226 (1970).
22. Ma, Y. *et al.* Genome-wide identification and characterization of novel genes involved in terpenoid biosynthesis in *Salvia miltiorrhiza*. *J Exp Bot* **63**, 2809–2823 (2012).
23. Hu, Y. T. *et al.* Cloning and bioinformatics analysis of *ent*-kaurene oxidase synthase gene in *Salvia miltiorrhiza*. *Zhongguo Zhong Yao Za Zhi* **39**, 4174–4179 (2014).
24. Tamura, K. *et al.* MEGA5: molecular evolutionary genetics analysis using maximum likelihood, evolutionary distance, and maximum parsimony methods. *Mol Biol Evol* **28**, 2731–2739 (2011).
25. Dai, Z. B. *et al.* Producing aglycons of ginsenosides in bakers' yeast. *Sci Rep* **4**, 3698 (2014).
26. Dai, Z. B. *et al.* Metabolic engineering of *Saccharomyces cerevisiae* for production of ginsenosides. *Metab Eng* **20**, 146–156 (2013).
27. Shi, M. Y. *et al.* Construction of *Saccharomyces cerevisiae* cell factories for lycopene production. *Zhongguo Zhong Yao Za Zhi* **39**, 3978–3985 (2014).
28. Zhang, M. *et al.* Identification of geranylgeranyl diphosphate synthase genes from *Tripterygium wilfordii*. *Plant Cell Rep* **34**, 2179–2188 (2015).
29. Sun, T. P. & Kamiya, Y. The Arabidopsis GA1 locus encodes the cyclase *ent*-kaurene synthetase A of gibberellin biosynthesis. *Plant Cell* **6**, 1509–1518 (1994).
30. Yamaguchi, S., Sun, T. P., Kawaide, H. & Kamiya, Y. The GA2 locus of Arabidopsis thaliana encodes *ent*-kaurene synthase of gibberellin biosynthesis. *Plant Physiol* **116**, 1271–1278 (1998).
31. van den Ent, F. & Lowe, J. RF cloning: a restriction-free method for inserting target genes into plasmids. *J Biochem Biophys Methods* **67**, 67–74 (2006).
32. Ukibe, K., Hashida, K., Yoshida, N. & Takagi, H. Metabolic Engineering of *Saccharomyces cerevisiae* for Astaxanthin Production and Oxidative Stress Tolerance. *Appl Environ Microbiol* **75**, 7205–7211 (2009).
33. Aslan, F. M., Yu, Y., Mohr, S. C. & Cantor, C. R. Engineered single-chain dimeric streptavidins with an unexpected strong preference for biotin-4-fluo. *Proc Natl Acad Sci USA* **102**, 8507–8512 (2005).
34. Green, L. S., Faergestad, E. M., Poole, A. & Chandler, P. M. Grain Development Mutants of Barley ([α]-Amylase Production during Grain Maturation and Its Relation to Endogenous Gibberellic Acid Content). *Plant Physiol* **114**, 203–214 (1997).
35. Morrone, D., Chen, X. M., Coates, R. M. & Peters, R. J. Characterization of the kaurene oxidase CYP701A3, a multifunctional cytochrome P450 from gibberellin biosynthesis. *Biochem J* **431**, 337–344 (2010).

Acknowledgements

This work was supported by the National Natural Science Foundation of China (81422053 and 81373906 to W.G. and 81325023 to L.H.) and National High Technology Research and Development Program of China (863 Program: 2015AA0200908) to W.G. and the Author of National Excellent Doctoral Dissertation of China (201188) to W.G.

Author Contributions

L.H. and W.G. conceived and designed the study. P.S. and Y.T. performed the experiments and wrote the manuscript. Q.C., Y.H., M.Z., J.Y. and Z.T. participated in the research and analyzed the data. All authors read and approved the final manuscript.

Additional Information

Supplementary information accompanies this paper at <http://www.nature.com/srep>

Competing financial interests: The authors declare no competing financial interests.

How to cite this article: Su, P. *et al.* Functional characterization of *ent*-copalyl diphosphate synthase, kaurene synthase and kaurene oxidase in the *Salvia miltiorrhiza* gibberellin biosynthetic pathway. *Sci. Rep.* **6**, 23057; doi:10.1038/srep23057 (2016).



This work is licensed under a Creative Commons Attribution 4.0 International License. The images or other third party material in this article are included in the article's Creative Commons license, unless indicated otherwise in the credit line; if the material is not included under the Creative Commons license, users will need to obtain permission from the license holder to reproduce the material. To view a copy of this license, visit <http://creativecommons.org/licenses/by/4.0/>